

Spin Polarization via Adiabatic and Counteradiabatic Engineering

Samuel Bladwell

School of Physics, University of New South Wales, Sydney 2052, Australia



(Received 31 December 2023; accepted 20 June 2024; published 25 July 2024)

A spin filter is a device that allows only a single spin state to pass, equivalent to a polarizing filter for a beam of light. Here, taking inspiration from shortcuts to adiabaticity, I demonstrate that the potential landscape of a typical quantum point contact can be tuned to act as a two terminal spin filter or to generate a spin-polarized beam. The effect presented is sufficiently robust that rough engineering yields a significant effect, as demonstrated by experiments on asymmetrically biased quantum point contacts in InAs quantum wells.

DOI: [10.1103/PhysRevLett.133.047001](https://doi.org/10.1103/PhysRevLett.133.047001)

Introduction—An electron spin filter or polarizer converts an unpolarized beam of electrons into a spin-polarized beam, equivalent to a polarizing filter for light. While such a device has been a topic of research interest ever since the discovery of spin, development of an apparatus to achieve this for electrons is not straightforward. Leon Brillouin, for example, proposed an electronic version of the Stern-Gerlach experiment to separate differing spin polarizations [1], however, as noted at the time, diffraction based broadening would make it impossible to separate the spin states using Brillouin’s proposal [2,3]. Much more recently, this persistent fundamental interest in spin-filtering electrons has been matched by technological drive, due to the proposal and demonstration of a variety of information processing devices where the information is encoded on the spin state of the charge carrier [4–6]. In such devices, spin polarizers and filters are critical components.

Fortunately, for spin-based information processing, creating a spin polarizer (or filter) in solid-state devices is less vexing than doing so in free space. Two approaches dominate. The first uses ferromagnetic contacts, where the large internal spin-splitting in the ferromagnet allows only one spin state to pass. The resulting current that is injected from the ferromagnetic contact to the device is spin polarized. The main drawback of this approach is the difficulty in integrating ferromagnetic contacts into semiconducting devices, both at the level of industrial fabrication and at the level of reliable spin injection. A second approach, which has seen an increasing interest over the past two decades attempts to avoid these difficulties via “all electric” spin filtering, where a combination of spin-orbit coupling and electron-electron interactions are employed, bypassing the need for ferromagnetic components [7,8]. These all-electric approaches have had varying success; while the need for ferromagnetic contacts is eliminated, the interaction induced gap is typically quite small, and the effect challenging to reliably implement.

In this Letter, I present an alternative approach to spin filtering and polarization, motivated by developments in “shortcuts to adiabaticity.” As its name suggests, shortcuts to adiabaticity aims to provide a shortcut to the otherwise slow time evolution of a Hamiltonian required for adiabatic evolution of states, via the addition of a driving term that suppresses the nonadiabatic transitions that would otherwise occur due to the rapid time evolution of the Hamiltonian [9–11]. This approach has already been employed extensively in quantum information science. Herein, I show how avoided crossings between spin-up and spin-down states of different subbands within a widening (or narrowing) waveguide can be used to achieve spin filtering, and how, by making use of the aforementioned design principle of shortcuts to adiabaticity, perfect spin polarization can be achieved. The presented approach can allow for high fidelity spin filtering and polarization. More remarkably, even quick and dirty approaches based on the method presented will yield a high degree of polarization. The effect is sufficiently robust that experimental groups have already inadvertently implemented this scheme of spin filtering.

Avoided crossing in quantum point contacts—A quantum point contact (QPC) is a quasi-one-dimensional constriction formed between two conducting reservoirs by applying a strong confining potential. This is typically done via a split gate, which depletes an underlying two-dimensional electron gas. While the lithographic dimensions are typically several times larger than the Fermi wavelength λ_F , the characteristic width W_0 of the constriction is comparable to the Fermi wavelength λ_F of the two-dimensional electron gas [12]. A schematic is presented in Fig. 1. The conductance of a QPC is characterized by a series of quantized conductance steps [13,14]. These conductance steps correspond to the reflectionless transport of electrons through the QPC potential. If the QPC is formed in a two-dimensional electron gas, where inversion symmetry is

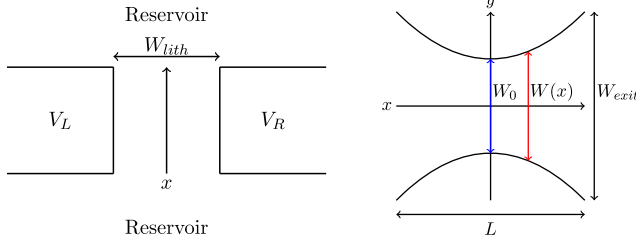


FIG. 1. Left panel: Schematic of a QPC. The regions above and below are the two-dimensional reservoirs, while the split gates have an applied potential V_L and V_R on the left and right, respectively. W_{lith} is the lithographic width of the split gates. Right panel: The potential profile of a QPC is characterized by a smoothly varying potential width, $W(x)$. The minimum width of the barrier is such that only the first subband can pass through, $W_0 \approx \lambda_F/2$, where λ_F is the Fermi wavelength.

broken by an applied electric field E_z in the growth direction of the quantum well, there will be a Rashba spin-orbit interaction

$$\mathcal{H}_R = \alpha_R(\hat{p}_x\hat{\sigma}_z - \hat{p}_y\hat{\sigma}_x), \quad (1)$$

where α_R parametrizes the strength of the Rashba interaction, and is proportional to E_z [15–17]. In narrow band gap semiconductor quantum wells, for instance, InAs, it can be up to 25% of the Fermi energy, and have a significant influence on the transport properties. Putting all these components together yields the Hamiltonian

$$\mathcal{H} = \frac{\hat{p}^2}{2m} + \alpha_R(\hat{p}_x\hat{\sigma}_z - \hat{p}_y\hat{\sigma}_x) + V(x, y), \quad (2)$$

where \hat{p} are the usual momentum operators and $V(x, y)$ is the potential of the QPC. The Hamiltonian, Eq. (2) will still display well-defined conductance steps, even for spin-orbit interactions $\sim 25\%$ of the Fermi energy [18]. These conductance steps will be in usual integer multiples of $2e^2/h$. So the quantum point contact is not spin resolved, and both spin states can pass through the constriction when a potential bias is created between the reservoirs even with very large spin-orbit interaction.

The dispersion of the subbands in the QPC is given by

$$E(n) = \varepsilon_n + \frac{p_x^2}{2m} \pm \alpha_R p_x, \quad (3)$$

where ε_n is the energy of the n th subband. If the confining potential in the y direction was parabolic, ε_n would be the energy levels of the harmonic oscillator, $\varepsilon_n = \hbar\omega_y(n + 1/2)$. The dispersion for two subbands is presented in Fig. 2. At a critical momentum, $p_x \approx (\varepsilon_2 - \varepsilon_1)/(2\alpha_R)$, the n th and $n + 1$ th subbands will anticross. This feature is shown in a cartoon in Fig. 2. While this crossing occurs at a specific value of momentum, there is no need to

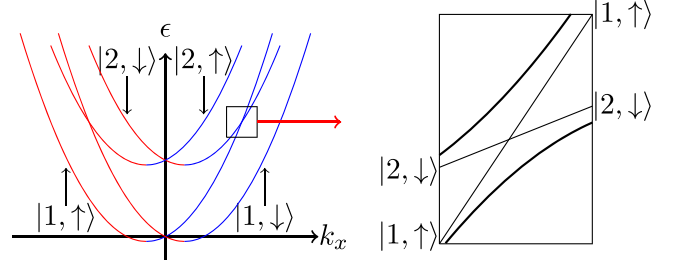


FIG. 2. Right panel: The dispersion of the one dimensional states for the lowest ($n = 1$) and second lowest ($n = 2$) subbands of the QPC, according to Eq. (3). Red (blue) indicates forward (backward) propagating states. At a particular k_x , $|1, \uparrow\rangle$ and $|2, \downarrow\rangle$ cross, highlighted in the boxed section. Only the forward propagating states (in blue) are relevant, due to current flowing in one direction. Left panel: Enlargement of the avoided crossing region. Thin lines indicate the crossing of the levels defined by the subband dispersion, Eq. (3).

tune the system to see this anticrossing. Provided the leads contain more subbands than the top of the potential barrier, at some point $x > 0$, there will be an anticrossing. So a QPC defined between two reservoirs, tuned to the first plateau will always have an anticrossing between subbands with different spin states.

I will be considering the anticrossing between the 1st and 2nd subbands. Rather than dealing with the 4×4 basis of the two subbands, I will consider a 2×2 subspace composed of the states that anticross, the spin-up state of the 1st subband $|1, \uparrow\rangle$, and the spin-down state of the 2nd subband $|2, \downarrow\rangle$:

$$\psi_a = |1, \uparrow\rangle = \phi_1(y) \begin{pmatrix} 0 \\ 1 \end{pmatrix}, \quad (4)$$

$$\psi_b = |2, \downarrow\rangle = \phi_2(y) \begin{pmatrix} 1 \\ 0 \end{pmatrix}. \quad (5)$$

Here, $\phi_n(y)$ is the transverse wave function. This approach has a fairly wide range of validity provided the Rashba interaction is large, due to the lack of terms mixing different subbands within the same spin branch; the full Hamiltonian consists of a series of 2×2 blocks. Having projected into this subspace, I am left with the following effective Hamiltonian,

$$\begin{aligned} \mathcal{H} &= \left(\frac{\hat{p}_x^2}{2m} - \varepsilon(x) \right) + (\alpha \hat{p}_x - \Delta(x))\tau_z - \alpha_R P_y \tau_y, \\ \varepsilon(x) &= \frac{\varepsilon_2 + \varepsilon_1}{2}, \quad \Delta(x) = \frac{\varepsilon_2 - \varepsilon_1}{2}, \\ P_y &= \langle 1 | \partial_y | 2 \rangle, \end{aligned} \quad (6)$$

describing the anticrossing region. I have introduced the energy $\varepsilon(x)$ and the gap $\Delta(x)$, the matrix element

$P_y = \langle 1|\partial_y|2\rangle$ over the spatial components of the subspace, along with the effective spin τ_i , which acts on the $(\psi_a, \psi_b)^T$ subspace. The position dependence of the energy and gap arises from the spatial dependence of the confining potential $V(x, y)$. If the effective width of the well varies in a sufficiently slow manner, the energy and gap can be treated as effective potentials [13].

The most informative way to look at Eq. (6) is as the sum of a kinetic and Zeeman term

$$\mathcal{H} = \mathcal{K} + \mathcal{B} \cdot \boldsymbol{\tau}, \quad (7)$$

where \mathcal{K} denotes the kinetic terms, and \mathcal{B} the effective field giving a Zeeman terms, and $\boldsymbol{\tau}$ is the effective spin composed of $|1, \uparrow\rangle$ and $|2, \downarrow\rangle$. These two terms can be considered separately, since the kinetic term is large and positive, while the effective field Zeeman term is small in the region about which \mathcal{B}_z vanishes. This makes it amenable to a semiclassical perturbative approach using the WKB wave functions. The semiclassical momentum is then

$$p(x) = \sqrt{2m(\varepsilon - \varepsilon(x))}, \quad (8)$$

which then yields the following effective magnetic field,

$$\mathcal{B} = (0, -\alpha_R P_y, \alpha_R p(x) - \Delta(x)). \quad (9)$$

The passage through the anticrossing region shown in Fig. 2 is represented by a rotation of this effective magnetic field. To make this more concrete, I take the unitary transform into the corotating frame,

$$\mathcal{U} = \exp\left(\frac{i\tilde{\theta}\tau_x}{2}\right), \quad (10)$$

$$\mathcal{H}' = \mathcal{U}\mathcal{H}\mathcal{U}^\dagger + i\frac{d\mathcal{U}}{dt}\mathcal{U}^\dagger, \quad (11)$$

where $\tilde{\theta}$ is the angle of the effective field \mathcal{B} and is a function of the position x . As the electron moves through the constriction of the QPC, it sees a rotation of this effective magnetic field, the rate of which is determined by the shape of the QPC. The second term added to the Hamiltonian comes from the time derivative of $\mathcal{U}\psi$. This term drives nonadiabatic transitions between the lower and upper states.

Making this term small requires a long, smooth QPC in conjunction with a very large spin-orbit interaction [18–21]. Obviously this is not ideal, as we would like to be able to shrink this term without onerous device requirements, and the purpose of the remainder of this Letter is to develop a method using the recently developed approach of shortcuts to adiabaticity red [9,11], by which the device can

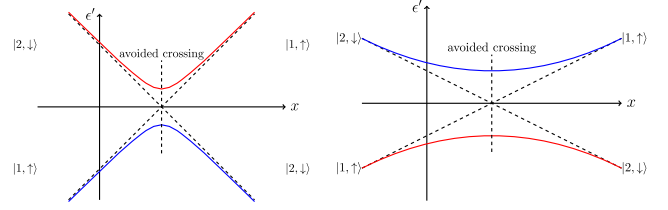


FIG. 3. Cartoons of the avoided crossing region, showing the effect of the asymmetric biasing of the QPC gates. The avoided crossing with symmetrically biased QPC gates (left panel) has a larger Landau-Zener velocity compared to asymmetrically biased QPC gates (right panel).

be tuned to act as a spin filter, without making it overly long, or the spin-orbit interaction unreasonably large.

Adiabatic engineering—Within the split-gate geometry of a QPC, applying an additional potential transverse to the channel of the QPC is fairly straightforward. The gates, rather than being symmetrically biased are biased at different voltages, V_1, V_2 . This introduces a transverse electric field, and breaks the inversion symmetry in the y direction. Laterally biased QPCs have been fabricated and tested many times, so such biasing does not constitute a significant technological challenge [7].

The effect of an applied transverse voltage is threefold. First, the resulting transverse electric field introduces an additional spin-orbit interaction. This has the form

$$\mathcal{H}_{\text{sol}} = \alpha_L(\sigma_y p_x) \quad (12)$$

and results in a canting of the spin within the QPC channel. Here α_L denotes the strength of the transverse spin-orbit interaction. [22] Within the literature is referred to as “lateral spin-orbit” coupling [7,23]. To account for additional spin-orbit terms, the unitary transformation is chosen to have an angle $\varphi = \tan^{-1}(\alpha_L/\alpha_R)$, while effective field \mathcal{B}_z now has a spin-orbit parameter, $\tilde{\alpha} = \sqrt{\alpha_L^2 + \alpha_R^2}$. Second, the asymmetric confinement also suppresses the gap term, $\Delta(x)$. To illustrate this point, I will consider the case of an additional potential created by a constant applied electric field, $\delta V(y) = eE_y y$. The resulting change to the gap in second order perturbation theory is

$$\delta\Delta = \frac{\delta\varepsilon_2 - \delta\varepsilon_1}{2} \approx -\frac{|\langle 1|eE_y y|2\rangle|^2}{\Delta}. \quad (13)$$

The combination of these two effects leads to a new \mathcal{B}_z , and moves the crossing region to smaller values of the effective momentum, $p(x)$. Since the rate of evolution of the angle of the effective field $\tilde{\theta}$ depends on the velocity with which the electron passes through the crossing region, the suppression of $p(x)$ reduces the diabatic term in Eq. (11). Third, the matrix element $P_y = \langle 1|\partial_y|2\rangle$ is enhanced. Again, in second order perturbation theory,

$$\delta P_y \approx P_y \frac{|\langle 1 | eE_y y | 2 \rangle|^2}{\Delta^2}. \quad (14)$$

In terms of effective fields, this enhances \mathcal{B}_y . Taking all of these effects together, the new effective field is

$$\mathcal{B} = (0, \alpha_R(P_y + \delta P_y), \tilde{\alpha}p(x) - (\Delta + \delta\Delta)). \quad (15)$$

These three effects form the static effects of the potential biasing of the QPC.

The applied electric field arises from the splits gates of the QPC being asymmetrically biased. Because of the strong screening of the in-plane components of the electric field by the reservoirs on either side of the split gates, the electric field resulting from the asymmetrical biasing will vanish near the edge of the QPC, much like the QPC potential itself. A simple estimate of the electric field is

$$E_y = \frac{V_R - V_L}{W(x)} \quad (16)$$

with $W(x)$ being the effective width of the QPC channel. The result of this varying electric field is a variation in the effective spin-orbit parameter, $\tilde{\alpha}$. On the other hand, $\delta\Delta$ varies only weakly with respect to the variation in the electric field, due to the approximate cancellation of the width dependence, as can be seen in Eq. (13).

Finally, using the values of the field from Eq. (15), I obtain the following value for the diabatic term in Eq. (11) at the level crossing, where \mathcal{B}_z vanishes:

$$i \frac{d\mathcal{U}}{dt} \mathcal{U}^\dagger \approx \frac{\tau_x}{\mathcal{B}_y} \frac{dx}{dt} \left[\frac{dp(x)}{dx} \tilde{\alpha}(x) + \frac{d\tilde{\alpha}(x)}{dx} p(x) + \frac{d\Delta}{dx} \right]. \quad (17)$$

And since $\tilde{\alpha}(x)$ and $\Delta(x)$ are decreasing functions, the sign of the derivatives are negative. By increasing the transverse electric field, the diabatic term can be tuned to vanish provided the gradient of the variation in $\tilde{\alpha}(x)$ is sufficiently large. A cartoon of the avoided crossing region, showing the effect of this asymmetrical biasing is presented in Fig. 3. However, the QPC has a finite length, and to maintain the position of the crossing within the channel of the QPC, $\alpha_L < \alpha_R$. Nonetheless, the fact that the degree of adiabaticity can be tuned means that we can enhance or suppress the spin polarization via an applied transverse potential.

Counterdiabatic engineering—In the general scheme of shortcuts to adiabaticity (STA), an additional term is engineered to cancel the diabatic term in Eq. (11). For many systems finding an approximate counterdiabatic control procedure is difficult, due to limited knowledge of the spectrum. Here, the difficulty is not working out what the appropriate control term is as the Hamiltonian is very simple. Rather the difficulty lies in finding an implementation in the QPC without unreasonable device

complications. From Eq. (11), the required additional term must be proportional to τ_x ,

$$i \frac{d\mathcal{U}}{dt} \mathcal{U}^\dagger = -\frac{\tau_x}{2} \frac{dx}{dt} \frac{d\tilde{\theta}}{dx}. \quad (18)$$

Fortunately, a τ_x term arises naturally from the QPC potential $V(x, y)$.

The spin-orbit interaction due to the QPC potential landscape variation in the x direction, that is, along the channel of the QPC, is

$$\mathcal{H}_{\text{SOP}} = -\gamma \frac{\partial V(x, y)}{\partial x} p_y \left(\frac{\alpha_R}{\tilde{\alpha}} \sigma_y + \frac{\alpha_Z}{\tilde{\alpha}} \sigma_z \right) \quad (19)$$

where I have introduced the spin-orbit parameter (SOP) γ , which is material dependent. The additional factors of α_R , α_Z , and $\tilde{\alpha}$ arise due to the canting of the spin from the applied transverse potential, and the resulting rotation of the spin-quantization axis in the QPC channel. While there is a term proportional to p_z , I am considering a quantum well, where the z confinement is very strong. Thus $\langle p_z \rangle = 0$. The combination of σ_y and p_y results in the following effective field term in the reduced basis given by Eq. (5),

$$\mathcal{H}_{\text{SOP}} = \mathcal{B}_x \tau_x = -\gamma \frac{\partial V(x, y)}{\partial x} P_y \tau_x \frac{\alpha_R}{\tilde{\alpha}(x)}, \quad (20)$$

where P_y is given by Eq. (14). Because of the smaller size of the QPC confinement potential, the strength of \mathcal{H}_{SOP} is less than that of the Rashba interaction. For a square well, based on the relative size of the confinement potential, this term can be up to 10% of the Rashba interaction [24]. By tuning the potential landscape $V(x, y)$, an exact cancellation of Eqs. (20) and (18) is possible. Achieving such cancellation is easier said than done. Small variations in the potential landscape $V(x, y)$ would add additional minor spin-orbit terms, and mix more distant subbands, making such global tuning extremely difficult in real devices.

On the other hand, local cancellation is considerably more straightforward. In this approach, cancellation is only between Eqs. (20) and (17). By tuning the transverse potential applied to the gates, Eq. (17) can be tuned without requiring any careful engineering of the potential landscape beyond that of a typical device. The sacrifice of this simpler approach is the degree of polarization attainable. Nonetheless, the effect is sufficiently robust that the polarization can easily be perfect with respect to experimental resolution, as is the case for QPCs formed in InAs quantum wells.

Experimental verification—A QPC normally displays quantized steps in conductance of $G = 2e^2/h$, e^2/h being the quantum of conductance; the factor of 2 from the two spin species. The usual experimental signature of spin

polarization in QPCs is a half step of $G = e^2/h$, half because only one spin makes it through the constriction. Numerous studies of spin polarization in QPCs have used this feature as a signature of spin polarization [7,8]. Unfortunately, this particular method of detecting spin polarization does not work for the aforementioned mechanism. Both spin states can pass through the constriction of the QPC, and the polarization occurs after this. Even when tuned to yield perfect polarization via this mechanism, a QPC will still display conductance steps of $G = 2e^2/h$. Far from being a drawback, with the appropriate detection setup this feature is beneficial, as it allows for a unique fingerprint of this particular mechanism of spin polarization. The key requirement is a method that is sensitive to the spin polarization of the emitted electrons. When the QPC is tuned to a conductance of $G = 2e^2/h$, the electron beam emitted by the QPC will still be spin-polarized, a feature that, in conjunction with the conductance steps, can only be explained by this mechanism.

One method for detecting the polarization of the QPC is transverse magnetic focusing, where the Rashba spin-orbit interaction required for the presence this mechanism of spin polarization also results in the spatial separation of the spin states [25,26]. The spatial separation then results in two peaks in the focusing spectrum, with the spin-polarization of the QPC resulting in the modulation of the relative height of the spin-split peaks [27]. In this setup, a QPC displaying the aforementioned mechanism will record a single transverse magnetic focusing peak even when the conductance of the source of QPC is $G = 2e^2/h$ [21].

Remarkably, there are already transverse magnetic focusing experiments that present this characteristic signature. In particular, transverse magnetic focusing has been used in InGaAs quantum wells featuring large spin orbit interactions, laterally biased QPCs as discussed in the previous section, and the characteristic spatial separation of the two spin-states [23,28]. At conductances of $G \leq 2e^2/h$, one of the spin-split focusing peaks is almost completely suppressed, with the double peak structure of an unpolarized source QPC restored only for $G > 3e^2/h$, the characteristic signature of this mechanism of spin filtering.

Recaptulation—I have presented a method, motivated by shortcuts to adiabaticity to tune a quantum point contact to act as a two terminal spin polarizer. In principle, exact engineering of the potential landscape can be used to achieve perfect spin polarization. A more immediately feasible approach is local engineering. This quick and dirty approach can still result in substantial spin polarization, and, moreover, seems to have been implemented incidentally in asymmetrically biased QPCs defined in InGaAs quantum wells, with a unique experimental signature in the transverse magnetic focusing spectrum. Most of all, the presented method of spin-filtering illustrates the value of shortcuts to adiabaticity in areas beyond quantum information science.

Acknowledgments—I would like to thank Oleg Sushkov for introducing me to the topic of transitionless quantum driving.

-
- [1] L. Brillouin, *Proc. Natl. Acad. Sci. U.S.A.* **14**, 755 (1928).
 - [2] N. F. Mott and N. H. D. Bohr, *Proc. R. Soc. A* **124**, 425 (1929).
 - [3] W. Pauli, Les theories quantities du magnetisme l'electron magnetique, in *Proceedings of the 6th Solvay Conference* (1930), pp. 183–186.
 - [4] S. Wolf, D. Awschalom, R. Buhrman, J. Daughton, S. Von Molnar, M. Roukes, A. Y. Chtchelkanova, and D. Treger, *Science* **294**, 1488 (2001).
 - [5] I. Žutić, J. Fabian, and S. D. Sarma, *Rev. Mod. Phys.* **76**, 323 (2004).
 - [6] S. Datta and B. Das, *Appl. Phys. Lett.* **56**, 665 (1990).
 - [7] P. Debray, S. Rahman, J. Wan, R. Newrock, M. Cahay, A. Ngo, S. Ulloa, S. Herbert, M. Muhammad, and M. Johnson, *Nat. Nanotechnol.* **4**, 759 (2009).
 - [8] M. Kohda, S. Nakamura, Y. Nishihara, K. Kobayashi, T. Ono, J.-i. Ohe, Y. Tokura, T. Mineno, and J. Nitta, *Nat. Commun.* **3**, 1082 (2012).
 - [9] M. Demirplak and S. A. Rice, *J. Phys. Chem. A* **107**, 9937 (2003).
 - [10] D. Guéry-Odelin, A. Ruschhaupt, A. Kiely, E. Torrontegui, S. Martínez-Garaot, and J. G. Muga, *Rev. Mod. Phys.* **91**, 045001 (2019).
 - [11] M. V. Berry, *J. Phys. A* **42**, 365303 (2009).
 - [12] H. van Houten and C. Beenakker, *Phys. Today* **49**, No. 7, 22 (1996).
 - [13] L. I. Glazman, G. B. Lesovik, D. E. Khmel'nitskii and R. I. Shekhter, *JETP Lett.* **48**, 238 (1988), http://jetpletters.ru/ps/1104/article_16696.shtml.
 - [14] B. J. Van Wees, H. Van Houten, C. W. J. Beenakker, J. G. Williamson, L. P. Kouwenhoven, D. F. Van der Marel, and C. T. Foxon, *Phys. Rev. Lett.* **60**, 848 (1988).
 - [15] R. Winkler, *Spin–Orbit Coupling Effects in Two-Dimensional Electron and Hole Systems*, Vol. 191 of Springer Tracts in Modern Physics (Springer Berlin Heidelberg, Berlin, Heidelberg, 2003), ISBN 978-3-540-01187-3, <http://www.springerlink.com/index/10.1007/b13586>.
 - [16] E. Rashba and E. Y. Sherman, *Phys. Lett.* **129A**, 175 (1988).
 - [17] Here I have rotated the Pauli matrices compared to the usual expression of the Rashba interaction by $U = \exp(i\pi\sigma_x/2)$.
 - [18] M. Eto, T. Hayashi, and Y. Kurotani, *J. Phys. Soc. Jpn.* **74**, 1934 (2005).
 - [19] M. Eto, T. Hayashi, Y. Kurotani, and H. Yokouchi, *Phys. Status Solidi C* **3**, 4168 (2006).
 - [20] P. G. Silvestrov and E. G. Mishchenko, *Phys. Rev. B* **74**, 165301 (2006).
 - [21] A. Reynoso, G. Usaj, and C. A. Balseiro, *Phys. Rev. B* **75**, 085321 (2007).
 - [22] As in the case of the Rashba interaction, Eq. (1), I have used the unitary rotation $U = \exp(i\pi\sigma_x/2)$ to rotate the Pauli matrices.
 - [23] S.-T. Lo, C.-H. Chen, J.-C. Fan, L. W. Smith, G. L. Creeth, C.-W. Chang, M. Pepper, J. P. Griffiths, I. Farrer, H. E. Beere *et al.*, *Nat. Commun.* **8**, 15997 (2017).

- [24] A. V. Moroz and C. H. W. Barnes, *Phys. Rev. B* **60**, 14272 (1999).
- [25] U. Zülicke, J. Bolte, and R. Winkler, *New J. Phys.* **9**, 355 (2007).
- [26] L. P. Rokhinson, V. Larkina, Y. B. Lyanda-Geller, L. N. Pfeiffer, and K. W. West, *Phys. Rev. Lett.* **93**, 146601 (2004).
- [27] S. Chesi, G. F. Giuliani, L. P. Rokhinson, L. N. Pfeiffer, and K. W. West, *Phys. Rev. Lett.* **106**, 236601 (2011).
- [28] P. Chuang, S.-C. Ho, L. Smith, F. Sfigakis, M. Pepper, C.-H. Chen, J.-C. Fan, J. Griffiths, I. Farrer, H. E. Beere *et al.*, *Nat. Nanotechnol.* **10**, 35 (2015).